Ni/γ-Al_2O_3 Catalyst Prepared by Liquid Phase Oxidation for Carbon Dioxide Reforming of Methane

Kyoung Soo Jung, Byoung-Youl Coh, and Ho-In Lee*

School of Chemical Engineering, Seoul National University, San 56-1, Shinlim-dong, Kwanak-ku, Seoul 151-742, Korea
Received October 22, 1998

Carbon dioxide reforming of methane on Ni/γ-Al_2O_3 catalyst was studied. A new 10 wt% Ni/γ-Al_2O_3 catalyst prepared by the liquid phase oxidation method (L10) exhibited much higher activity as well as resistances to both sintering and coke formation during the reaction than the catalyst prepared by the conventional impregnation method (D10). The electrically strong attractive interaction between nickel and support during the liquid phase oxidation process and the resultant high nickel dispersion made the L10 have superior activity and stability to the D10. To elucidate the results, the experiments with nickel catalysts on the other supports as well as γ-Al_2O_3 were performed. The effect of sodium as a promoter was also studied.

Introduction

There has recently been a renewed interest in carbon dioxide reforming of methane, a process which was originally studied by Fischer and Tropsch in 1928. Carbon dioxide reforming of methane has an industrial advantage over steam reforming of methane because the former produces synthesis gas ($CO+H_2$) which contributes to the feed for Fischer-Tropsch synthesis with the hydrogen-to-carbon monoxide ratio of unity which is desirable for the synthesis network to produce higher hydrocarbons and oxygenated derivatives.[1,2]

$CH_4 + H_2O \rightarrow CO + 3H_2$ ($\Delta H = 226$ kJmol^{-1})
: steam reforming of methane
$CH_4 + CO_2 \rightarrow 2CO + 2H_2$ ($\Delta H = 261$ kJmol^{-1})
: carbon dioxide reforming of methane

The reaction has an environmentally important implication because both methane and carbon dioxide, which are greenhouse gases to bring about global warming,[3~6] can simultaneously be converted to useful gases.

A major problem in carrying out this reaction is the deactivation of catalyst due mainly to carbon deposition *via* Boudouard reaction ($2CO \rightarrow C+CO_2$) and/or methane decomposition ($CH_4 \rightarrow C+2H_2$) both of which are favorable under the reaction conditions. In recent years, efforts have been focused on the development of catalysts which show high activity and resistance to coking. Supported noble metal catalysts[7~11] were found to be promising in terms of the methane conversion and resistance to coking as compared to the nickel-based catalysts. However, considering the aspects of high cost and limited availability of noble metals, it is more practical to develop some improved nickel-[12] or cobalt-[5,13] based catalysts which exhibit stable operation. In particular, the recent research has been focused on nickel catalysts.

Lanthanum oxide-[14,15] or zeolite-[16] supported nickel catalysts were found not to be much sensitive to coke formation. On the other hand, γ-Al_2O_3 was reported to be a poor support for nickel catalyst used in this reaction, in terms of the methane conversion and resistances to both sintering and coking.[14,15,17-19]

In this study, however, the results were obtained over Ni/γ-Al_2O_3 catalyst prepared by liquid phase oxidation,[20] a new process of catalyst preparation, which gave high activity and excellent stability for the catalyst.

Experimental Section

Preparation of Catalyst. Ni/γ-Al_2O_3 catalysts were prepared via conventional impregnation and liquid phase oxidation, respectively. The details of the two preparation methods are as follows: (1) Conventional Impregnation; γ-Al_2O_3 (JRC-ALO-2) was impregnated to an aqueous solution of nickel nitrate ($Ni(NO_3)_2 \cdot 6H_2O$: Junsei Chemical Co.) at 80 keeping pH of 5. After most of the water was evaporated, the remaining paste was dried at 120 °C for more than 12 hours resulting in a supported nickel catalyst (DX). "D" means that the catalyst experienced the above drying process after impregnation step, and "X" indicates the amount of nickel loaded on γ-Al_2O_3 by weight percent. (2) Liquid Phase Oxidation; powdered DX was oxidized in an NaOH + NaOCl aqueous solution with pH of 13 at 80 °C. The instantaneous change of color of the powder from green (DX) to black was observed. The black precipitate was inferred as NiOOH where the oxidation state of nickel is +3 suggesting that the nickel species with the oxidation state of +2 existed in DX was oxidized by NaOCl, a strong oxidizer. NaOH functioned as a precipitant. This black precipitate was washed fully to remove sodium off and was dried at 120 °C for more than 12 hours. The nickel catalyst obtained in this way was termed LX. "L" implies that the catalyst experienced the liquid phase oxidation step.

*To whom all correspondence should be addressed. e-mail: hilee@plaza.snu.ac.kr

10 wt% Ni catalysts with other supports than γ-Al_2O_3 were prepared. D10/SiO_2, D10/TiO_2, D10/ZnO, and D10/MgO were made by conventional impregnation and L10 catalysts with these metal oxides as supports were also prepared by liquid phase oxidation.

Finally, 10 wt% Ni/γ-Al_2O_3 catalysts doped with Na were made by conventional impregnation. 1, 5, 10, and 50 wt% of Na were doped by co-impregnation with nickel nitrate using sodium nitrate as a sodium precursor.

Catalytic Reaction. Activity measurements were carried out in a fixed-bed continuous-flow reactor made of 1/4 inch i. d. quartz tube. The catalyst were pretreated with H_2 just before the reaction. That is, the powdered catalyst was heated from room temperature to 700 °C and then cooled down to room temperature with H_2/N_2 in the reactor. The standard catalytic reaction condition was reaction temperature of 700 °C, CH_4/CO_2 of 1, and catalyst amount of 20 mg. The effluent gas was analyzed with a gas chromatograph using Porapak Q as a separating column.

Characterization of Catalyst. The chemical and physical properties of the catalysts were analyzed. The redox properties of the catalysts were studied by temperature-programmed reduction (TPR) method using a TCD cell. Nickel dispersions and BET surface areas of the catalysts were measured by H_2 chemisorption at room temperature in a vacuum system evacuated by a rotary pump, and N_2 adsorption, respectively. The coke deposited on the used catalyst was analyzed by both CHN analysis and TPR.

Results and Discussion

Catalytic Activity. Figure 1 shows the catalytic activities expressed as methane conversion at 700 °C and the nickel dispersions measured by H_2 chemisorption of the D10 and the L10 as a function of reaction time. The D10, which showed about 60% of initial methane conversion, lost

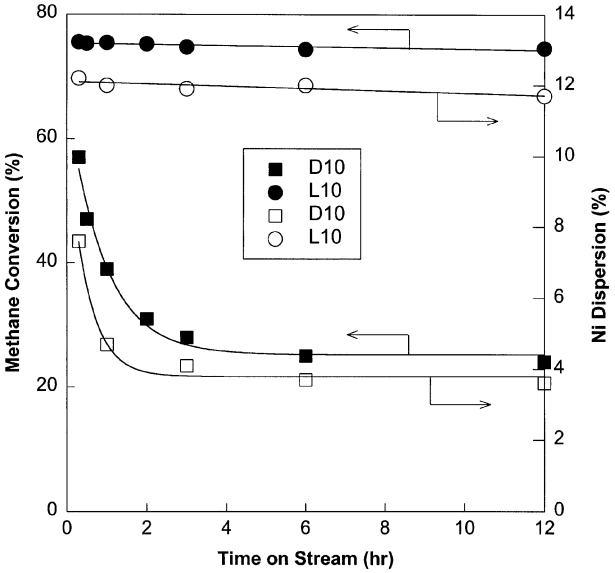

Figure 1. Methane conversion at 700 °C and nickel dispersion over the D10 and the L10 as a function of reaction time.

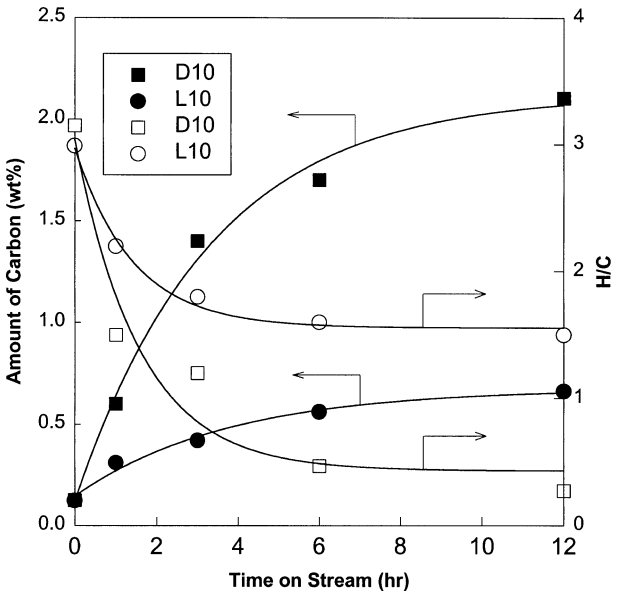

Figure 2. Variations of carbon deposited and H/C ratio on the D10 and the L10 as a function of reaction time at 700 °C.

sharply its activity at the beginning of the reaction reaching the steady state conversion, less than the half of the initial value within 3 hours, while the L10 exhibited high activity above 70% and stability for a long period of reaction time. In case of the D10, the nickel dispersion of the fresh catalyst was 7.6%, but within a few hours it went sharply down to almost its half. The L10, on the other hand, which showed relatively high dispersion of the fresh catalyst as 12.2%, scarcely suffered any loss of its nickel dispersion for first 12 hours of the reaction. The higher dispersion of the fresh L10 than the fresh D10 accounts for the higher initial activity of the L10 in Figure 1, and it can be seen that only the D10 was sintered during the reaction resulting in deactivation. The reason why the D10 was deactivated will be discussed later.

Coke Formation. Figure 2 shows the amount of coke deposited and the ratio of hydrogen to carbon (H/C) on the catalyst surface measured by CHN analysis as a function of reaction time at 700 °C. On the D10, much more coke was deposited and the H/C ratio went down more sharply than on the L10. During the catalytic reaction the coke from the hydrocarbons like methane formed through the processes like these:[21]

$$CH_4 \rightarrow CHx + \frac{4\text{-}x}{2} H_2 \text{ (decomposition of methane)}$$

$$CH_4 \rightarrow C + \frac{x}{2} H_2 \text{ (dehydrogenation)}$$

After CHx, the precursor of the coke, was formed on the catalyst surface by the decomposition of methane, the formation of graphitic carbon proceeded through the dehydrogenation of CHx. Therefore, the lower H/C ratio of the D10 suggests that relatively more graphitic carbon was deposited on the surface of the D10 during the reaction than on that of the L10. That is, the poisoning due to coke deposition on the D10 went worse than on the L10.[22] Although the methane

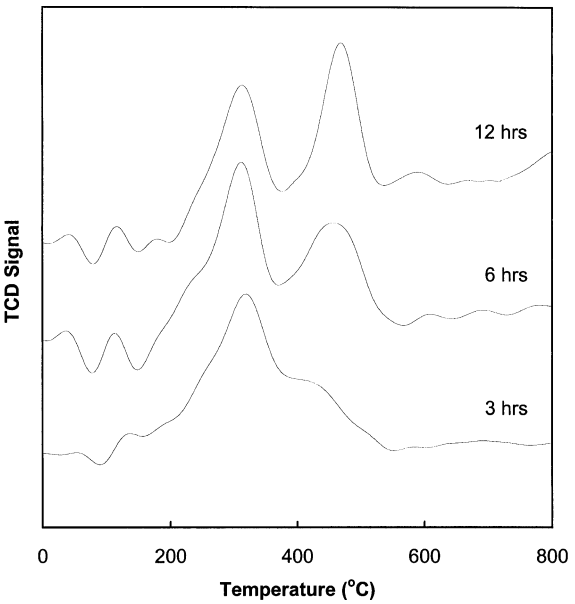

Figure 3. TPR spectra of the D10 after three different reaction times at 700 °C.

conversion and Ni dispersion of the D10 did not show further decreases after 3 hours of reaction time, the amount of carbon deposited on the surface of the D10 increased with respect to reaction time suggesting that the decrease of Ni dispersion was the main factor for catalyst deactivation rather than carbon deposition.

Figures 3 and 4 represent the TPR spectra of the used D10 and L10 after three different reaction times, respectively. The peaks in the TPR curves of the used catalysts correspond to the formations of methane ($C + 2H_2 \rightarrow CH_4$) and a small amount of ethane ($2C + 3H_2 \rightarrow C_2H_6$) by the hydrogenation of carbon species on the catalyst surface.[23] The carbon species formed during the reaction can be separated into two: The one desorbed at about 300 °C and the other desorbed above 400 °C. The latter might be deposited on the surface with stronger attractive force and thus functioned as severer poison than the former. For the catalysts used for 3 hours, most of the coke on the surface of the L10 was desorbed at about 300 °C with a little amount of the carbon desorbed above 400 °C, whereas the peak above 400 °C appeared clearly on the D10. And on the D10, the height of the peak above 400 °C increased more rapidly than on the L10 as the reaction proceeded showing higher peak temperature by about 40 °C on the D10. The result also shows that the poisoning due to coke deposition was worse on the D10 than on the L10. The discussion will be given later. Meanwhile, the TPR peak areas of the D10 after 3 hours of reaction time and of the L10 after 12 hours were similar to each other although the L10 showed much higher catalytic activity than the D10. This can be explained in terms of Ni dispersion as discussed earlier. That is, the catalytic activity is suggested to depend strongly on the dispersion of metal much rather than the deposition of carbon.

Characterization of Catalyst. From the results presented above, it is shown that the L10 having higher nickel dispersion showed higher catalytic activity and resistances to both the sintering and coke deposition during the reaction than the D10. To account for this, the TPR experiments were performed. Figure 5 represents the TPR spectra of the fresh D10 and L10 catalysts. The peak at about 200 °C in case of the L10, corresponds to the reduction of Ni^{3+} in NiOOH formed by liquid phase oxidation to Ni^{2+}. The peak around 300 °C comes from the reduction of bulk nickel oxide which is not associated with the support, and that over 400 °C, the reduction of the surface and near surface nickel ($Ni^{2+} \rightarrow Ni^0$), which actually contributes to the catalytic reaction. Thus, in case of the D10, most of the nickel existed as bulk state resulting in poor nickel dispersion and activity. On the other hand, the majority of the nickel was well dis-

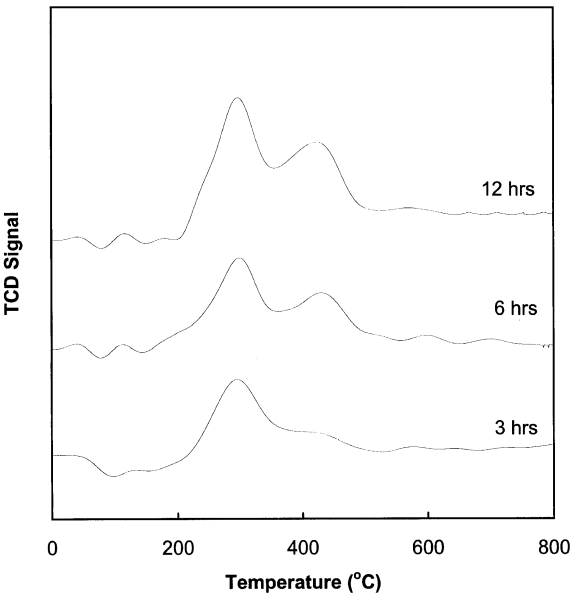

Figure 4. TPR spectra of the L10 after three different reaction times at 700 °C.

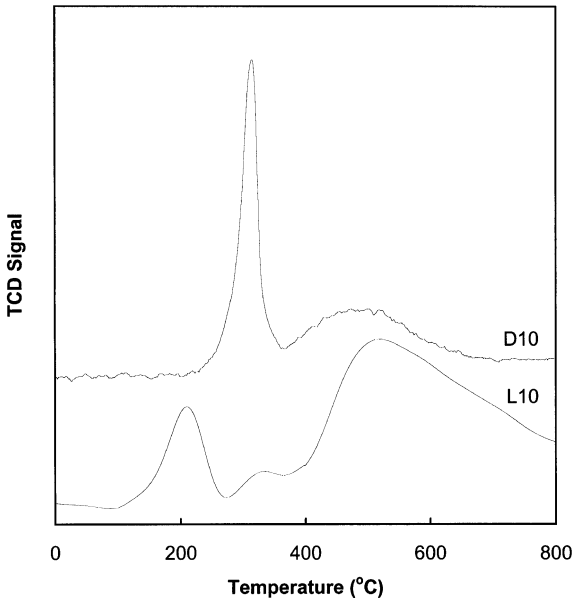

Figure 5. TPR spectra of the fresh D10 and L10.

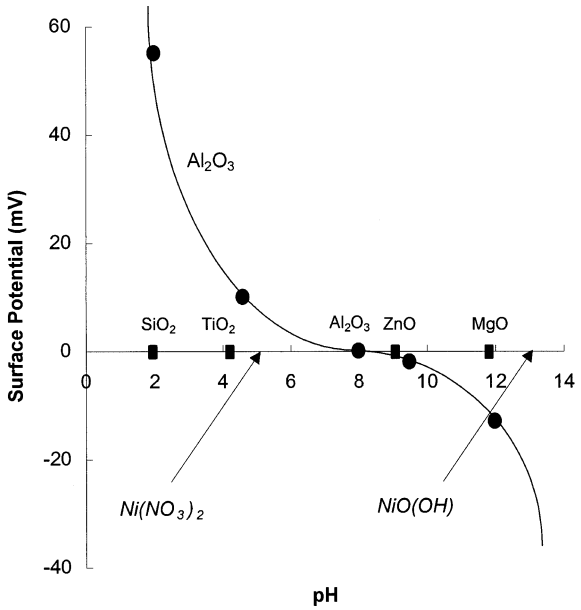

Figure 6. Surface potential of Al_2O_3 as a function of PH, and isoelectric points of some metal oxides.[25]

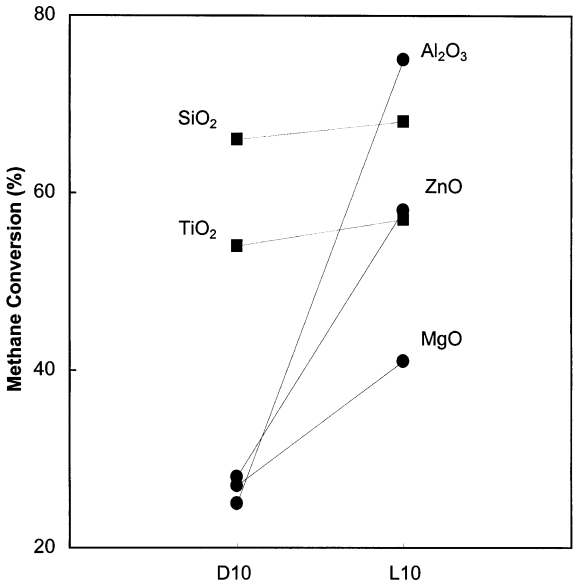

Figure 7. Steady-state methane conversion over the D10 and the L10 supported on various metal oxides.

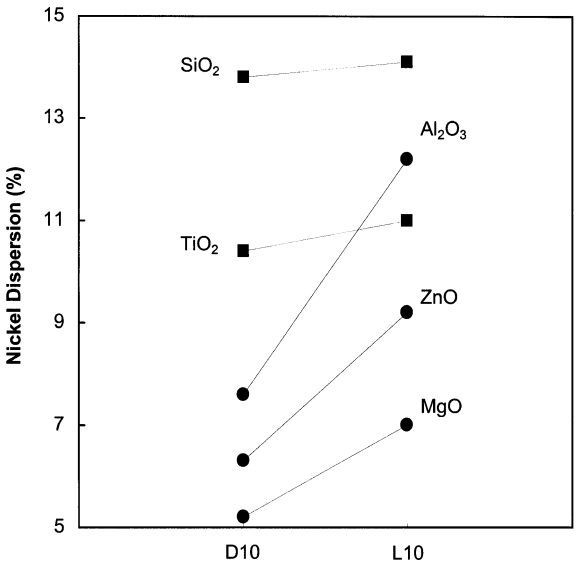

Figure 8. Nickel dispersion of the D10 and the L10 supported on various metal oxides.

persed on the surface of γ-Al_2O_3 showing high activity in case of the L10.

The reason why the L10 with higher dispersion was more resistant to coke deposition than the D10 can be explained by the carbon deposition model suggested by Erdohelyi *et al.*[24] According to the model on Rh/Al_2O_3 catalyst, the coke on Rh can move to the support just as hydrogen on the metal spills over. When the dispersion of Rh was high, this spillover of surface carbon easily occurred because the nickel particle was small, and as a result, the Rh surface could participate freely in the reaction for a long period of reaction time without a significant coke formation. The coke which migrated to the support could react with CO_2 which was readily adsorbed on the support to produce CO *via* the reverse Boudouard reaction ($C + CO_2 \rightarrow 2CO$). Thus, only if the metal size was small, the overall coke formation on the surface decreased and the catalyst could be highly resistant to the deactivation by coking. Just as the Rh catalyst, the L10 with much higher nickel dispersion could exhibit higher resistance to coke deposition than the D10.

Interaction between Nickel Precursor and the Support. The electrical interaction between nickel precursor and the support during impregnation and liquid phase oxidation explains the higher activity and stability of the L10 than the D10. Figure 6 represents the isoelectric points and the surface potentials of some metal oxides which are generally used as support.[25] The surface charge of a metal oxide changes from positive (+) through zero (0 : isoelectric point) to negative (-) as the pH increases. At pH below the isoelectric point, therefore, the surface is positively charged, and vice versa. When γ-Al_2O_3 is used as a support, the electrical interactions between nickel and the support in cases of the D10 and the L10 can be explained as follows: Because the nickel precursor ($Ni(NO_3)_2$) has its oxidation state of +2 and the surface of the support having its isoelectric point at around pH 8 is positively charged at pH 5, weak electrical repulsive force exists between nickel and the support in the impregnation step at pH 5. On the other hand, in the liquid phase oxidation step, because the oxidation number of the nickel precursor changes from +2 to +3 and the surface of the support is negatively charged at pH 13, relatively strong electrical attractive force between them can make nickel exist more stickily on the support. Therefore, the stronger interaction between nickel and the support in the L10 accounts for its higher nickel dispersion and activity as well as its higher resistances to sintering and coking than the D10.

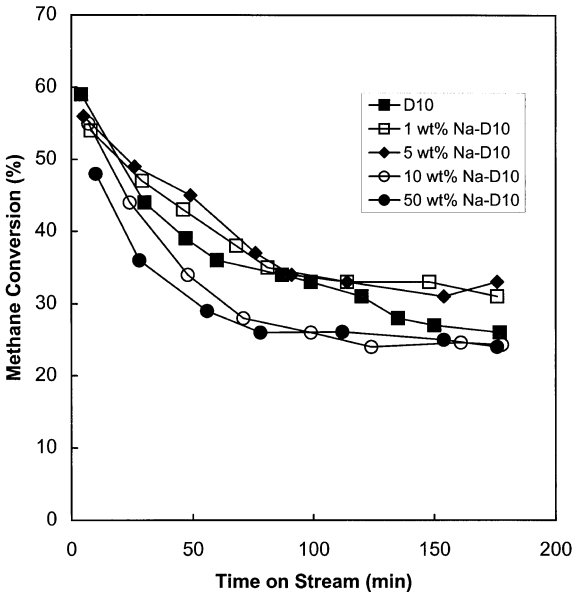

Figure 9. Methane conversion over 10wt% Ni/γ-Al_2O_3 doped with various amounts of Na.

To elucidate the explanation described above, other metal oxides like ZnO, MgO, TiO_2, and SiO_2 were used as supports for the nickel catalyst. Figures 7 and 8 represent the steady state methane conversions and nickel dispersions of the nickel catalysts supported on various metal oxides, respectively. The increases in both the activity and the nickel dispersion by liquid phase oxidation were greater for the catalysts with γ-Al_2O_3, ZnO, and MgO as supports than for those with TiO_2 and SiO_2 as supports.

As seen in Figure 6, γ-Al_2O_3, ZnO, and MgO have their own isoelectric points between pH 5 and pH 13 suggesting that the surfaces of these metal oxides have negative charge when the impregnation step proceeds at pH 5 and positive one when the liquid phase oxidation step takes place at pH 13. As mentioned above, therefore, due to the electrical interactions between nickel and the metal oxides, the liquid phase oxidation affected greatly on both activity and nickel dispersion. On the other hand, in cases of TiO_2 and SiO_2 as supports, because their isoelectric points existed below pH 5, the increases in the electrical interactions between nickel and the supports and the resultant increases in activity and nickel dispersion by liquid phase oxidation were not so significant.

Effect of Sodium. It can be considered that the enhancement in nickel dispersion, and the resultant catalytic activity and stability by liquid phase oxidation might be caused by the addition of sodium as a promoter into the solution of NaOH + NaOCl. In fact, for many catalytic reactions, the addition of alkali metal such as sodium showed positive effect in both activity and stability[26~29] suggesting that the experiment about the effect of sodium is needed.

Figure 9 shows the effect of sodium on the activity of the 10 wt% Ni/γ-Al_2O_3 catalyst made by conventional impregnation. With the addition of sodium upto 5 wt%, the activity increased slightly, and further addition gave rather a negative effect on the activity due to the blocking of active sites rather than modification. The addition of sodium did not show a significant positive effect on the activity unlike expectation.

Conclusions

10 wt% Ni/γ-Al_2O_3 catalyst for carbon dioxide reforming of methane prepared by the liquid phase oxidation method, a new method of catalyst preparation (L10), exhibited much higher catalytic activity as well as resistances to both sintering and coke formation during the reaction than the catalyst prepared by the conventional impregnation method (D10). The electrically strong attractive interaction between nickel and support during the liquid phase oxidation step at pH 13 and the resultant high nickel dispersion made the L10 have superior activity and stability to the D10. The nickel catalysts supported on ZnO and MgO, which had their own isoelectric points between pH 5 and pH 13 just like γ-Al_2O_3, also exhibited the enhancement in activity and stability by liquid phase oxidation, while in case of the nickel catalysts supported on TiO_2 and SiO_2 whose isoelectric points are located below pH 5, the increases in activity and stability by the process were not so significant.

Acknowledgement. This work was supported by the S. N. U. Posco Research Fund. The authors would like to thank both S. N. U. for financial support and The Catalysis Society of Japan for supplying alumina as a support.

References

1. Trimm, D. L. *Catal. Rev. Sci. Eng.* **1997**, *16*, 155.
2. Aparicio, L. M. *J. Catal*. **1997**, *165*, 262.
3. Blom, R.; Dahl, I. M.; Slagtern, A.; Sortland, B.; Spjelkavik, A.; Tangstad, E. *Catal. Today* **1994**, *21*, 535.
4. Inui, T. *Catal. Today* **1996**, *29*, 329.
5. Osaki, T.; Masuda, H.; Horiuchi, T.; Mori, T. *Catal. Lett*. **1995**, *34*, 59.
6. Osaki, T.; Horiuchi, T.; Suzuki, K.; Mori, T. *J. Chem. Soc., Faraday Trans.* **1996**, *92*, 1627.
7. Ashcroft, A. T.; Cheetham, A. K.; Green, M. L. H.; Vernon, P. D. F. *Nature* **1991**, *352*, 225.
8. Rostrup-Nielsen, J. R.; Bak Hansen, J.-H. *J. Catal*. **1993**, *144*, 38.
9. Nakamura, J.; Aikawa, K.; Sato, K.; Uchijima, T. *Catal. Lett.* **1994**, *25*, 265.
10. Basini, L.; Sanfilippo, D. *J. Catal*. **1995**, *157*, 162.
11. Bitter, J. H.; Hally, W.; Seshan, K.; van Ommen, J. G.; Lercher, J. A. *Catal. Today* **1996**, *29*, 349.
12. Gadalla, A. M.; Bower, B. *Chem. Eng. Sci*. **1988**, *43*, 3049.
13. Guerrero-Ruiz, A.; Rodriguez-Ramos, I.; Sepulveda-Escribano, A. *J. Chem. Soc., Chem. Commun.* **1993**, 487.
14. Zhang, Z.; Verykios, X. E. *J. Chem. Soc., Chem. Commun*. **1995**, 71.
15. Zhang, Z.; Verykios, X. E. *Catal. Lett.* **1996**, *38*, 175.
16. Chang, J.-S.; Park, S.-E.; Chon. H. *Appl. Catal. A:General* **1996**, *145*, 111.
17. Gadalla, A. M.; Sommer, M. E. *Chem. Eng. Sci*. **1989**, *44*, 2825.

18. Yamasaki, O.; Nozaki, T.; Omata.; Fujimoto, K. *Chem. Lett.* **1992**, 1953.
19. Zhang, Z. L.; Verykios, X. E. *Catal. Today* **1994**, *21*, 589.
20. Nakagawa, K.; Konaka, R.; Nakata, T. *J. Org. Chem.* **1962**, *34*, 1597.
21. Richardson, J. T. *Principles of Catalyst Development*; Plenum Press: New York, U. S. A., **1989**; p 210.
22. Nishijima, A.; Shimada, H.; Yoshimura, Y.; Sato, T. *Stud. Surf. Sci. Catal.* **1987**, *34*, 39.
23. Kroll, V. C. H.; Swaan, H. M.; Mirodatos, C. *J. Catal*. **1996**, *161*, 409.
24. Erdohelyi, A.; Cserenyi, J.; Solymosi, F. *J. Catal*. **1993**, *141*, 287.
25. Reed, J. S. *Introduction to the Principles of Ceramic Processing*; North-Holland: New York, U. S. A., **1991**; Ch. 9.
26. Campbell, J. M.; Nakamura, J.; Campbell, C. T. *J. Catal*. **1992**, *136*, 24.
27. Clake, D. B.; Bell, A. T. *J. Catal*. **1995**, *154*, 314.
28. Driscoll, S. A.; Gardner, D. K.; Ozkan, U. S. *Catal. Lett*. **1994**, *25*, 191.
29. Lim, K.-C.; Lee, G. D.; Lee, H.-I. *J. Kor. Ind. Eng. Chem*. **1992**, *3*, 722.